American Mineralogist, Volume 70, pages 885–901, 1985

TEM study of a pyroxene-to-pyroxenoid reaction

DAVID R. VEBLEN

Department of Earth and Planetary Sciences
The Johns Hopkins University, Baltimore, Maryland 21218

Abstract

A specimen of the CaMn clinopyroxene johannsenite that has partially reacted to Mn pyroxenoids has been studied with high-resolution transmission electron microscopy (HRTEM), electron diffraction, and single-crystal X-ray methods. The primary johannsenite is structurally ordered pyroxene, and the end product of the reaction is relatively well-ordered rhodonite. Intermediate products include pyroxmangite (siebenerketten), rhodonite (fünferketten), and unit-cell level mixtures of the pyroxmangite and rhodonite structures. These disordered mixed materials have variable average structures and contain rare lamellae with ordered sequences of fünferketten and siebenerketten.

Regardless of the intermediate structure involved, these solid-state reactions can take place either by lamellar or bulk mechanisms, similar to replacement mechanisms reported for other silicate reactions. The ways in which the pyroxene and pyroxenoid structures can fit together control in part which reaction mechanisms can occur.

One of the observed reaction paths, from johannsenite to pyroxmangite to rhodonite, is unusual because rhodonites generally contain more calcium than coexisting pyroxmangite with low Fe and Mg. Therefore, rhodonite might be expected to form before pyroxmangite in a reaction series involving loss of calcium; thus, the growth of pyroxmangite in this occurrence may be metastable. One unresolved problem involves the observation that in relatively large regions of pyroxene, lamellae of pyroxenoid appear to nucleate and grow in only one of two symmetrically equivalent orientations. This orientational selectivity may result from templating on pyroxenoid on the grain boundaries or from the involvement of shear in the reaction.

Introduction

The pyroxenoids and pyroxenes comprise a homologous series of single-chain silicates. The chains of pyroxenes have a periodicity of two tetrahedra, and pyroxenoids, because their chains are offset in various ways, have periodicities of 3, 5, 7, or 9 tetrahedra (these are referred to as dreierketten, fünferketten, siebenerketten, and neunerketten pyroxenoids, respectively; see Liebau, 1962, 1980; Prewitt and Peacor, 1964). Alternatively, pyroxenes and pyroxenoids have been viewed as a polysomatic series consisting of different sequences of wollastonite (W) and pyroxene (P) slabs, cut parallel to (011) of pyroxene (Koto et al., 1976; Takéuchi and Koto, 1977; Narita et al., 1977; Thompson, 1978).

Burnham (1966) speculated that in addition to perfectly periodic pyroxenoids, there might exist pyroxenoids with mistakes in the periodicity of the chain offsets. Such mistakes, now referred to as "chain periodicity faults" (Czank and Liebau, 1980), have been recognized in several recent high-resolution transmission electron microscopy (HRTEM) studies of both natural and synthetic pyroxenoids (Czank and Liebau, 1979, 1980; Ried et al., 1979; Ried and Korekawa, 1980; Alario Franco et al., 1980; Jefferson et al., 1980; Jefferson and Pugh, 1981; Czank, 1981; Czank and Simons, 1983; Aikawa, 1984). In the polysomatic model, these chain periodicity faults can be viewed as mistakes in the sequence of W and P slabs.

Although chain periodicity faults clearly are relatively abundant in some pyroxenoids, there were no reports of the analogous faults in pyroxenes until recently. Veblen (1982) and Ried (1984) now have reported chain periodicity disorder in natural pyroxenes, and Catlow et al. (1982) synthesized pyroxene–pyroxenoid mixtures. The present HRTEM study of a johannsenite specimen that has partially reacted to the Mn pyroxenoids rhodonite (fünferketten) and pyroxmangite (siebenerketten) expands our understanding of chain periodicity disorder and related faults in both pyroxenes and pyroxenoids. More important, because these pyroxenoids formed by reaction from primary pyroxene, this study provides us with a clear picture of the solid-state mechanisms of reaction. The reaction of johannsenite to pyroxenoids has long been recognized as a common one. In fact, it was first reported by Schaller (1938) in his original description of johannsenite as a new mineral. Angel et al. (1984) recently provided a theoretical discussion of pyroxene-pyroxenoid reactions, in part relying on experimental observations from an earlier draft of the present paper. Preliminary reports of this work are given by Veblen (1982) and in Buseck et al. (1980).

0003–004X/85/0910–0885$02.00

Specimen description and experimental techniques

The specimen employed in this investigation was collected from a Mn-rich skarn in the Govedarnika polymetallic deposit, District of Luki, northern Rhodope Mountains, Bulgaria, by Prof. Donald M. Burt, who kindly made it available for study. The Govedarnika deposit has been described by Stoinova and Pirov (1974).

In the hand specimen used in this study, a metasomatic zonation is apparent, in which a zone of olive-colored pyroxene is replaced by a zone of gemmy pink pyroxenoid. In thin section, the pyroxene occurs in obvious sprays (Fig. 1a). As noted by Burt, the pyroxene has been partially replaced, forming feathery intergrowths with pyroxenoid (Fig. 1b). Chemically, this replacement involves removal of Ca and Fe and addition of Mn.[1] The pink pyroxenoid that replaces these intergrowths appears in the petrographic microscope to be crystallographically continuous with the pyroxene, and in many cases one can observe that a single "crystal" grades from virtually unreplaced pyroxene at one end, through intergrown pyroxene and pyroxenoid, to the gemmy pink pyroxenoid at the other end.

Single-crystal X-ray diffraction experiments performed with a precession camera indicate that the gemmy pink pyroxenoid is mostly rhodonite, with only minor amounts of intergrown pyroxmangite. Streaking parallel to $\mathbf{c}^*$ indicates some disorder in chain periodicity but is not intense. Lamellar features resulting from the intergrowth of this minor pyroxmangite and chain periodicity faulting can be seen in thin section and in oil mounts in the petrographic microscope, although the intergrowth is on a scale too fine to permit identification of specific areas as pyroxmangite. The intergrowth also results in changes in extinction angle within individual "crystals." The observed angle between the **c**-axis and the (001)[2] lamellae of about 68° is consistent with the identification of the bulk of this material as rhodonite.

Specimens for the TEM study were prepared by ion milling pieces of petrographic thin section. Only the feathery intergrowths of pyroxene and pyroxenoid were examined with electron microscopy. The specimens were lightly coated with carbon. Electron microscopy was performed with a JEOL JEM 100B microscope operated at 100 kV, as described by Veblen and Buseck (1979).

TEM studies of chain periodicity faults in pyroxenoids, noted above, primarily have involved imaging of the 00*l* diffractions. Therefore, for intergrown pyroxenoids and clinopyroxenes, one might at first suppose that imaging of the (011) pyroxene planes would best reveal the intergrowth features. However, since the 011 diffractions are forbidden by the pyroxene *C*-centering, and the spacing of the (022) planes (2.23Å) is less than the resolution of the microscope used in this study, this approach is rather futile. Furthermore, it was found in this study that pyroxenoid lamellae in most cases did not form parallel to the pyroxene (011) planes, but instead parallel to $(11\bar{1})$. Therefore, most microscopy was performed with the electron beam parallel to $[1\bar{1}0]$. In this orientation, both the $11\bar{1}$ pyroxene diffractions and 00*l* diffractions from $(11\bar{1})$ pyroxenoid lamellae contribute to HRTEM images, as well as diffuse intensity scattered by disordered arrays of chain periodicity faults in the pyroxene. Even when the $(11\bar{1})$ periodicity in pyroxene is not resolved, the (110) planes and the (001) pyroxenoid periodicity generally can be observed, and chain periodicity faults produce interpretable contrast.

[1] A preliminary X-ray analytical study of the intergrowths in the TEM indicates the following approximate compositions:

johannsenite: $Ca_{0.9}Mn_{0.8}Fe_{0.3}Si_{2.0}O_6$

pyroxenoids: $Ca_{0.6}Mn_{1.3}Fe_{0.1}Si_{2.0}O_6$

A more thorough analytical TEM study of the different ordered and disordered pyroxenoids described in this paper is in progress to determine whether there is a statistically valid difference in composition between the different reaction products. Analyses were obtained with a Phillips 420ST microscope equipped with an EDAX detector and a Princeton Gamma-Tech analyzer, using silicate standards.

[2] The *C*-centered ($C\bar{1}$) unit cell setting, as used by Ohashi and Finger (1975), is used for the pyroxenoids throughout this paper.

Chain periodicity order and disorder

Relatively large regions of the pyroxene in this specimen (tens of microns in extent) can possess perfect chain periodicity order, as exhibited by the electron diffraction pattern and lattice image of johannsenite (Jo) in Figure 2. This structurally ordered material, with chain periodicity 2, presumably represents the state in which the pyroxene grew as a primary skarn mineral. Likewise, regions of relatively well-ordered rhodonite (Rh) and pyroxmangite (Pmg) also occur (Fig. 2). However, these minerals in all cases were observed to contain at least some chain periodicity faults, mostly of the siebenerketten-type in rhodonite and both the fünferketten and neunerketten types in pyroxmangite. No dreierketten faults were observed in either pyroxene or pyroxenoid.

The pyroxene, rhodonite, and pyroxmangite can be identified by their characteristic diffraction patterns and the periodicities of HRTEM images as shown in Figure 2, and this interpretation of contrast can be extended to HRTEM images of disordered intergrowths. Specifically, the $(11\bar{1})$ spacing of johannsenite (4.5Å) can be differentiated from the (001) spacings of rhodonite (11.4Å) and pyroxmangite (15.8Å), even in images of disordered chain silicate, and longer periodicities can be attributed to chain repeats longer than seven (e.g., the neunerketten (001) spacing of 20.3Å). Such interpretation methods are consistent with those used in previous HRTEM studies of disordered pyroxenoids, as noted above.

Much of the chain silicate in this specimen cannot be categorized as any of the classically defined pyroxenoids, but instead is a disordered mixture of different chain periodicites, especially five and seven. An example of such material is shown in Figure 3, which consists of an apparently random mixture of these two common repeats. Intimate mixtures of rhodonite and pyroxmangite were reported by Sundius (1931), who called the intergrown material "sobralite." Such mixtures were most recently studied by Aikawa (1979, 1984) and Ried and Korekawa (1980). The image of Figure 3 shows that the scale of such intermixing can extend down to the unit cell level.

In addition to completely disordered chain periodicity sequences, short runs of long-period ordered sequences were observed. Of these, two structures passed the significance test of Veblen and Buseck (1979) at the $p < 0.001$ level. The sequence (557) was observed in one case to repeat six times ($p = 3.3 \times 10^{-4}$) and in another place to repeat eight times ($p = 8.6 \times 10^{-6}$). Five unit cells of the

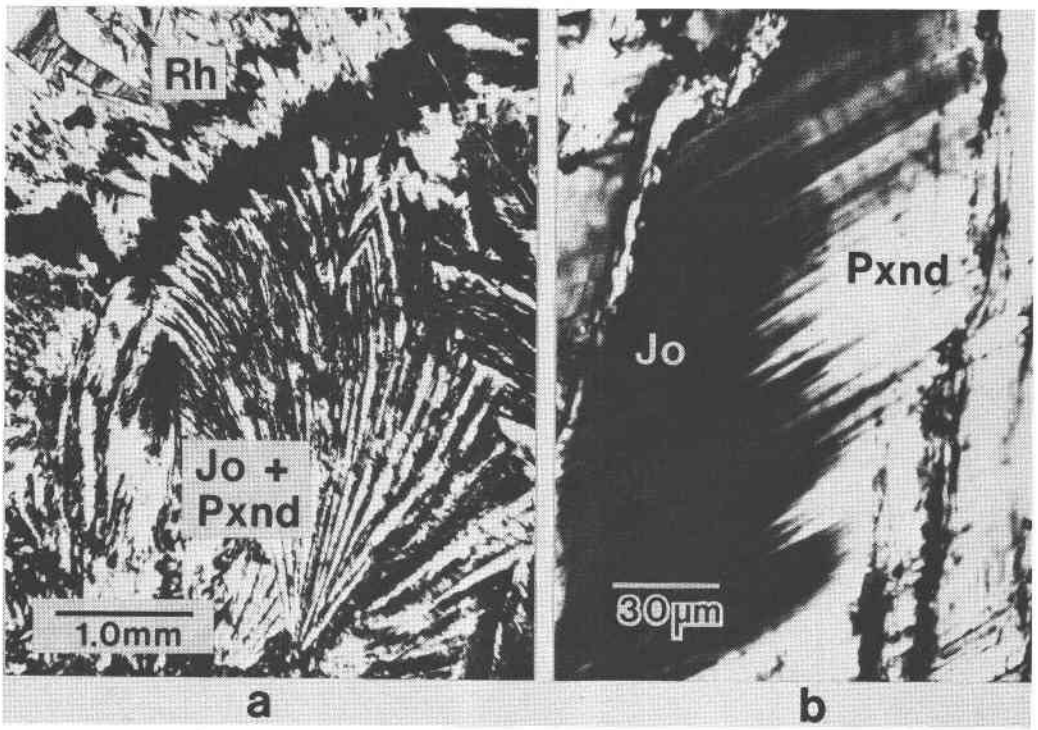

Fig. 1. a. A spray of johannsenite crystals that have been partially replaced by pyroxenoid (Jo + Pxnd). At the top, relatively well-ordered rhodonite (Rh) has replaced the other chain silicates completely. Crystal elongation is parallel to **c**. (Plane polarized light.) b. A feathery intergrowth of johannsenite with pyroxenoid. The pyroxene **c**-axis is vertical. (Cross polarized light, with the johannsenite at extinction.) Note difference in scale between a and b.

sequence (57557) were also observed ($p = 7.9 \times 10^{-6}$). Five repeats of the sequence (557) are shown in Figure 4. Sequences that are apparently non-random, such as (557) and (57557), might result from a tendency of siebenerketten units to repel each other when immersed in a fünferketten matrix. This would be analogous to the behavior of crystallographic shear planes in reduced non-stoichiometric oxides such as WO_{3-x} (Iguchi and Tilley, 1978).

The different types of pyroxene and pyroxenoid intergrowths that are present in this specimen produce a variety of electron diffraction patterns, as shown in Figure 5. Since these patterns were recorded from specimen areas larger than one micron, they provide information about the average structures of different types of intergrowths. Figure 5a is a diffraction pattern from ordered johannsenite, as in Figure 1, for reference. The diffraction pattern in Figure 5b is from an area of johannsenite with extensive chain periodicity faulting and intergrowth of disordered fünferketten-siebenerketten pyroxenoid. This disorder results in the heavy streaking parallel to the pyroxenoid **c*** direction. The presence of sharp pyroxene diffractions (which can be seen by comparison with Fig. 5a) indicates that the johannsenite occurs in relatively large blocks. Figure 5c is from a region of intergrown pyroxmangite and johannsenite. Again, relatively sharp pyroxene diffractions are superimposed on the more prominent pyroxenoid pattern. Light streaking parallel to the pyroxenoid **c*** results from minor chain periodicity disorder in the pyroxmangite.

Diffractions from pyroxene do not appear in the electron diffraction patterns of Figures 5d–f, which are from areas with little or no johannsenite. Figure 5d is typical of areas of five and seven units in disordered arrangements, as shown in Figure 3. The sharper diffractions of Figures 5e and f are in nonintegral positions with respect to the ordered structures of this pyroxene–pyroxenoid system. Such nonintegral patterns typically occur in intergrowth structures where there is an imperfect periodicity of the different structural units (Cowley, 1975, p. 150; Buseck and Cowley, 1983). These structures could be considered to be modulated structures based on intergrowth of five- and seven-repeat structural units, for example.

The electron diffraction patterns of Figure 5 emphasize the fact that the complex chain silicate specimen employed in this study contains not only ordered pyroxene and pyroxenoids, but also a variety of disordered materials with a range of average structures. In this section we have been concerned only with the description of these various structures. In the next section we will discuss the reactions that produced them.

Intergrowth details and reaction mechanisms

As noted above, the primary chain silicate that formed during skarn crystallization was presumably ordered johannsenite, as characterized by sharp electron diffraction

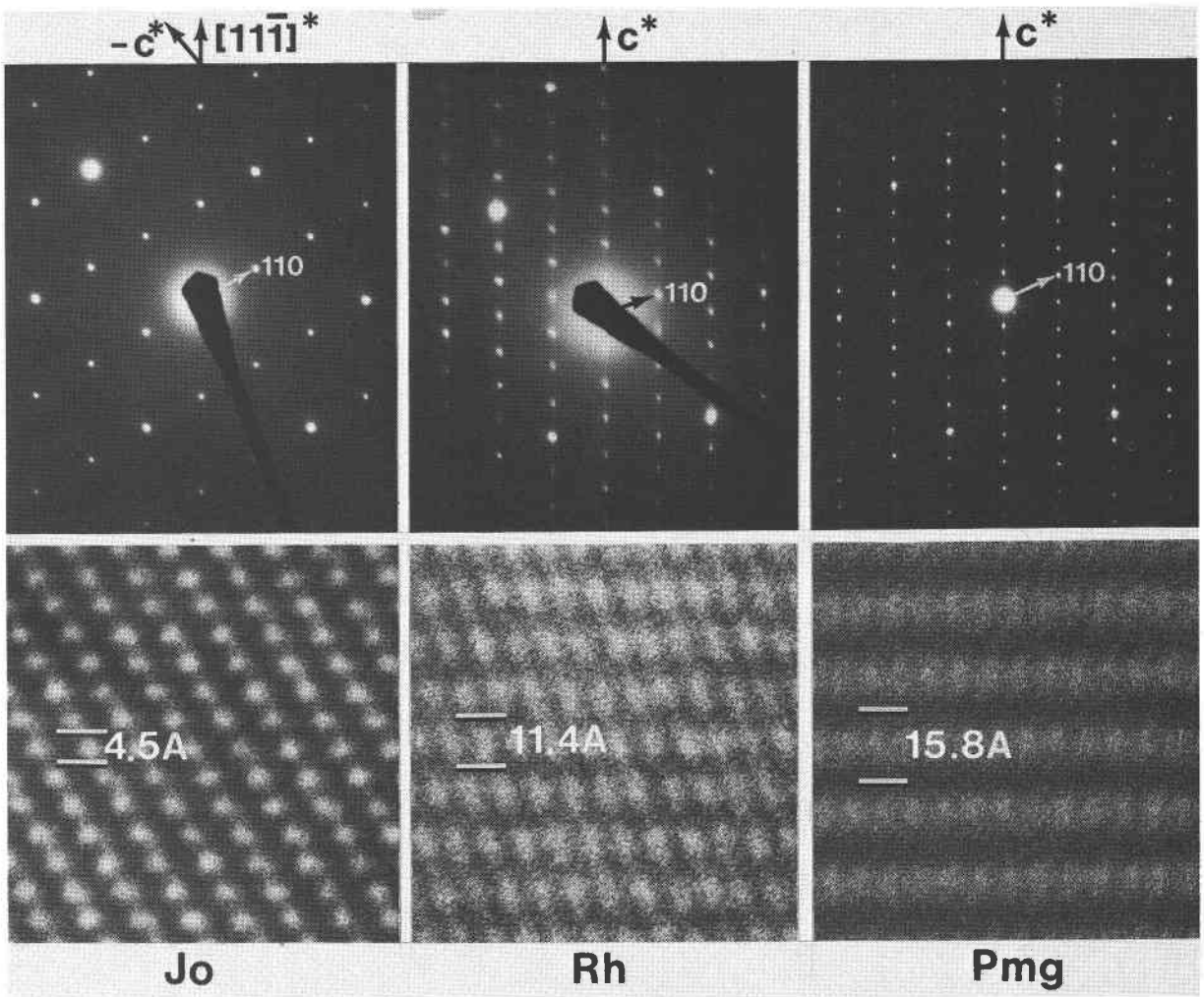

Fig. 2. Electron diffraction patterns and HRTEM images of johannsenite (Jo), rhodonite (Rh), and pyroxmangite (Pmg). The rhodonite and pyroxmangite diffraction patterns exhibit weak streaking parallel to c* from minor chain periodicity disorder. The johannsenite image is on a slightly larger scale than those of the pyroxenoids.

patterns like the one in Figures 2 and 5a. The mechanisms of the solid-state reactions that produced the ordered pyroxenoids and disordered intergrowths described in the last section can be deduced by examining the microstructural details of the partially reacted materials.

Lamellar reactions

Figure 6 shows a common texture found in johannsenite that is in close proximity to material that has reacted more completely in pyroxenoid. The pyroxene contains narrow lamellae of pyroxenoid (arrowed) that are parallel to (11$\bar{1}$) and spaced roughly 1000Å apart, on the average. Although these lamellae are generally quite continuous, in some cases they are observed to terminate (two terminations are indicated by the white arrows in Fig. 6). It thus appears that pyroxene can be converted at least partially to pyroxenoid by the nucleation and growth of narrow pyroxenoid lamellae (or chain periodicity faults). We refer to such a mechanism as a lamellar reaction mechanism.

A more detailed view of several lamellae of rhodonite structure in pyroxene is shown in Figure 7a. The lamellae, indicated as "5," can be either paired or isolated. The expanded view of an isolated rhodonite unit in Figure 7b shows that the lamella has finite width, i.e., that the pyroxene chains are offset along two chain periodicity fault planes (arrowed) that are five tetrahedra apart. Such a structure, viewed normal to (100), is diagrammed in Figure 8, which shows the chains of a rhodonite lamella that ter-

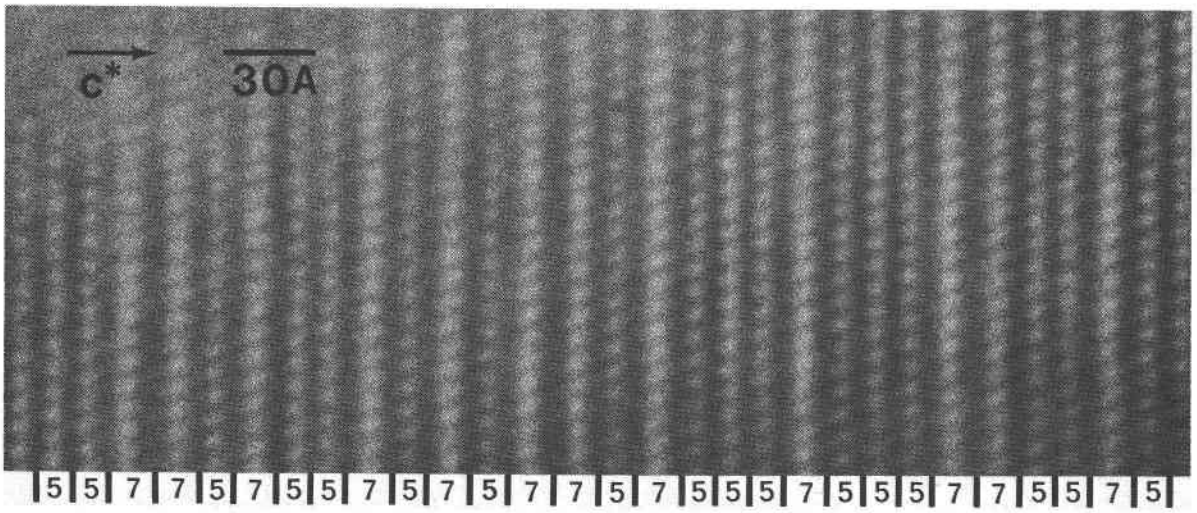

Fig. 3. A HRTEM image of disordered pyroxenoid with both 5 and 7 tetrahedra between chain offsets (i.e., a mixed rhodonite-pyroxmangite structure). Rhodonite-like slabs are labelled "5," and pyroxmangite-like slabs are designated "7."

minates in normal pyroxene.[3]

Isolated chain periodicity faults were not observed in this specimen. This is presumably because a single offset cannot be introduced into the pyroxene without producing considerable strain or a nonsensical structure at the termination of the fault, as shown in Figure 9. On the other hand, a pair of offsets can be introduced coherently, with little strain, to produce a lamella of rhodonite (Fig. 8) or other pyroxenoid structure. These structural constraints on the formation of pyroxenoid lamellae in pyroxene can be formalized in a simple rule: a $(11\bar{1})$ or (011) pyroxenoid lamella that terminates in unstrained pyroxene must contain an even number of chain offsets; if the lamella contains an odd number of offsets termination will involve considerable strain or displacive planar faults. This geometrical rule is analogous in many ways to the two termination rules formulated by Veblen and Buseck (1980) for chain-width errors in pyriboles. Although the octahedral strips may impose additional constraints on these lamellar reactions, it is not necessary to consider them in deriving this termination rule. The octahedral strips have been discussed in some detail by Angel et al. (1984).

The fact that all observed pyroxenoid lamellae in the pyroxene of this specimen contained at least two chain offsets supports the notion that the nucleation and growth of a single offset produces considerable strain and is therefore energetically unfavorable. In addition, this observation strongly suggests that the pyroxenoid lamellae are, indeed, secondary, postcrystallization features, since there is no reason to expect that chain periodicity faults formed during crystal growth always would be paired. However, the absence of isolated chain periodicity faults in the johannsenite should not be taken to imply that the pyroxenoid lamellae are in all cases coherently intergrown with the pyroxene, with essentially no strain involved. Figure 10, for example, is from a region exhibiting extreme strain contrast around part of a pyroxenoid lamella that contains several planes of chain offset. Furthermore, while many narrow pyroxenoid

[3] A note on terminology for faults in the pyroxene–pyroxenoid polysomatic series is required. In this paper I use the term offset (or single offset) to refer to the kink in the silicate chains of a single W slab as used by Thompson (1978), except that the W slabs in the present specimen lie in $\{11\bar{1}\}$, rather than {011} as supposed by Thompson. I refer to lamellae having five tetrahedra between offsets as lamellae of rhodonite structure or fünferketten lamellae, even though the detailed chemistry of a given lamella may differ from that of bulk rhodonite (obviously, these isolated lamellae haven't been analyzed, and the exact atom positions are not known). Likewise, I call lamellae having seven tetrahedra between offsets pyroxmangite or siebenerketten lamellae.

In pyroxenoids, a lamella of anomalous chain periodicity is referred to as a single chain periodicity fault. Thus, a lamella of pyroxmangite structure embedded in rhodonite host would be a single chain periodicity fault. This is logical in the context of the polysomatic model for these structures, since such a fault results from the introduction of a single extra P slab (in the sense of Thompson, 1978). In the pyroxene structure, however, a slab of rhodonite structure results from the introduction of *two* anomalous slabs, in this case W slabs. I therefore refer to such a lamella as consisting of two chain periodicity faults. A single extra W slab inserted into pyroxene structure is a perfectly possible type of fault. This would not correspond to a fault of rhodonite structure, or pyroxmangite structure, or the structure of any other pyroxenoid. To avoid having to call such a fault a half chain periodicity fault, it is necessary to refer to each anomalous P or W slab as a single chain periodicity fault, when these slabs are not adjacent. A neunerketten fault in rhodonite, for example, which consists of two adjacent extra P slabs, could still be called a single chain periodicity fault, following the usage of Czank and Liebau (1980), Czank and Simons (1983), and other workers.

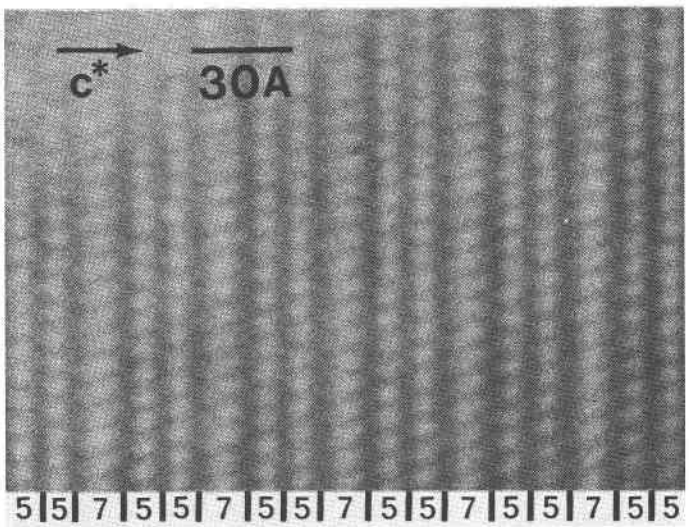

Fig. 4. An ordered sequence (557) of mixed rhodonite and pyroxmangite structures. Five unit cells in the direction of ordering are shown.

lamellae contain an even number of offsets, as in Figures 7b and c, some contain an odd number (three or greater), as shown in Figure 7d, where there are three planes of chain offset.

Pyroxenoid lamellae with an odd number of chain offsets could form in either of two ways. First, it is possible that they could nucleate and grow in the primary pyroxene as isolated lamellae with considerable strain associated with their terminations. This might be possible because the strain would be distributed over more of the structure than in the case of the nucleation and growth of a single, isolated chain periodicity fault. However, such terminations exhibiting strong strain contrast have not been observed.

The second way in which pyroxenoid lamellae with an odd number of offsets could form is by the nucleation and growth of cooperatively terminating lamellae connected by planar faults, analogous to the cooperative growth of chain-width errors in pyriboles (Veblen, 1981; Veblen and Buseck, 1980). Growth of the lamellae would entail motion of the planar faults through the structure. Such faults connecting the terminations of narrow pyroxenoid lamellae occur in some parts of the specimen. One such region is shown in Figure 11a, where the vertical pyroxenoid lamellae are sharp, because they are oriented parallel to the electron beam, whereas the planar faults connecting the lamellar terminations show diffuse banded contrast typical of stacking faults that are tilted with respect to the electron beam. The faults are presumably either stacking faults or polysomatic defects, depending on orientation (see also discussion below). HRTEM images demonstrate that the projected displacements across such faults are variable.

Excellent TEM images of planar faults similar to those shown in Figure 11a have been presented previously by Ried and Korekawa (1980, e.g., Fig. 2). These faults were in synthetic pyroxenoids, rather than in pyroxene with isolated pyroxenoid lamellae. Czank (1981, e.g., Fig. 5) showed high-resolution images of analogous planar defects in babingtonite. Planar faults of this type were likewise observed in the pyroxenoids of the present study. Figure 11b shows one such fault in pyroxmangite. Chain periodicity faults are terminated by the planar fault, which meanders across the figure. A very localized displacive fault is shown in Figure 11c; the fault displaces an elferketten (11-repeat) slab in pyroxmangite.

A high-resolution image of cooperatively-terminating pyroxenoid lamellae in pyroxene is shown in Figure 12. Each of the lamellae contains several planes of chain offset (i.e., several pyroxenoid repeats). The lamellae are connected by planar faults, which are easily seen because the surrounding structure has been rendered amorphous as a result of enhanced electron radiation damage. Formation and growth of such cooperatively terminating lamellae, as well as simply terminating lamellae, appear to be important mechanisms of pyroxene-to-pyroxenoid reaction.

In some areas, pyroxenoid lamellae have largely replaced the pyroxene, but some pyroxene remains as narrow lamellae separated by pyroxenoid. An example is shown in Figure 13, where remnant pyroxene appears as bright white stripes, and the pyroxenoids pyroxmangite and rhodonite are darker gray. This figure also shows dark blotches that are produced by electron radiation damage. These are concentrated on the lamellar interfaces, indicating that the damage is preferentially nucleated at these sites, presumably because the interface energies are higher than those of the bulk structures.

Figure 14 shows a high-resolution image of the pyroxenoid typical of an area like that in Figure 13. Both pyroxmangite and rhodonite are present, with the large rhodonite lamella in the center of the figure terminating in the pyroxmangite. The pyroxmangite contains abundant chain peridocity faults, some of which are offset in several places or terminate in normal pyroxmangite. There are also

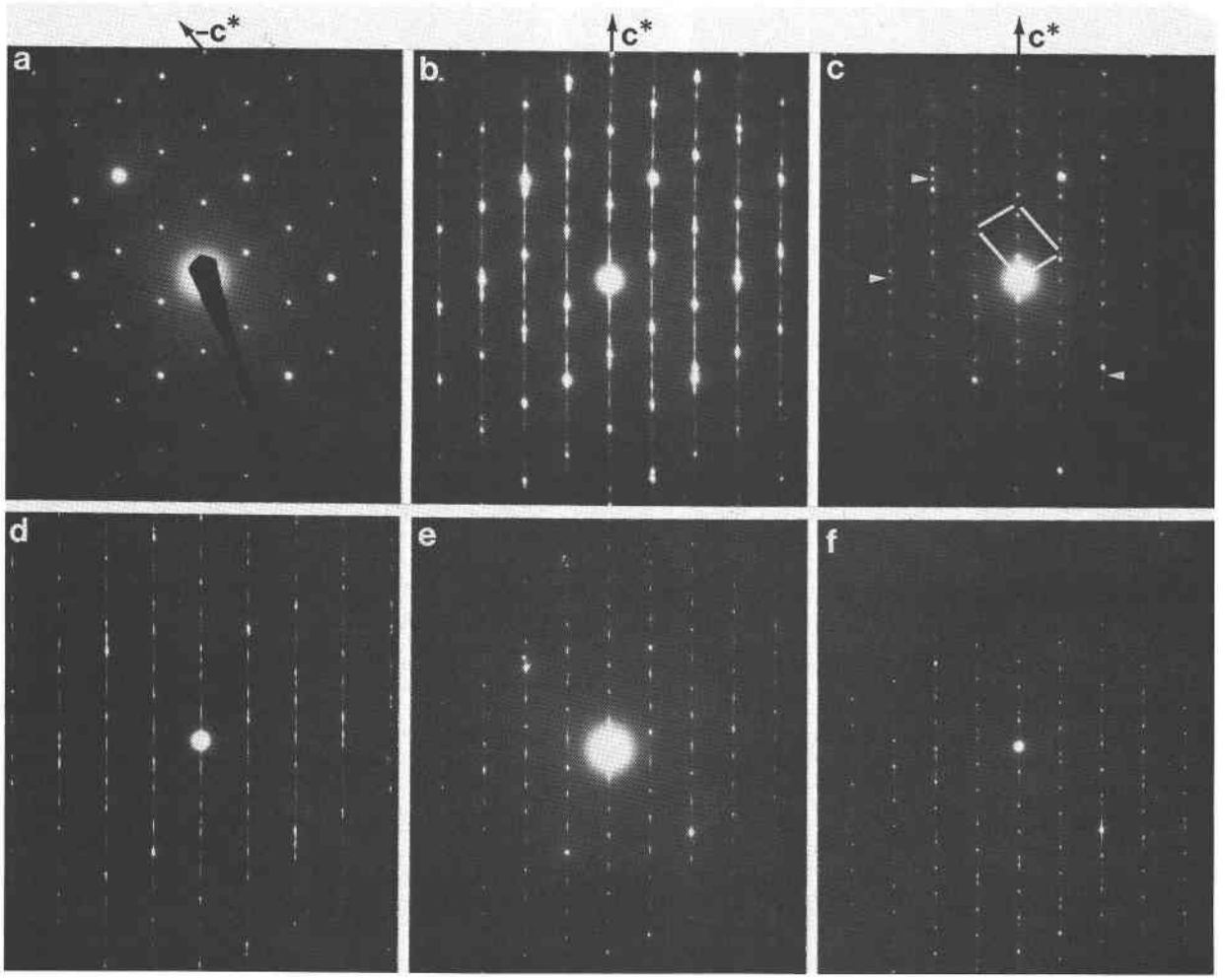

Fig. 5. Electron diffraction patterns taken parallel to [1$\bar{1}$0]. a. Ordered johannsenite. b. Partially reacted johannsenite with extensive chain periodicity disorder. c. Relatively well-ordered pyroxmangite with some remnant johannsenite. The most prominent pyroxene diffractions are arrowed, and a pyroxene cell formed by the $-c^*$ and [110]* translations is outlined. d. Pyroxenoid with extreme chain periodicity disorder. e, f. Two examples of disordered pyroxenoid with average structures that produce relatively sharp non-integral diffractions.

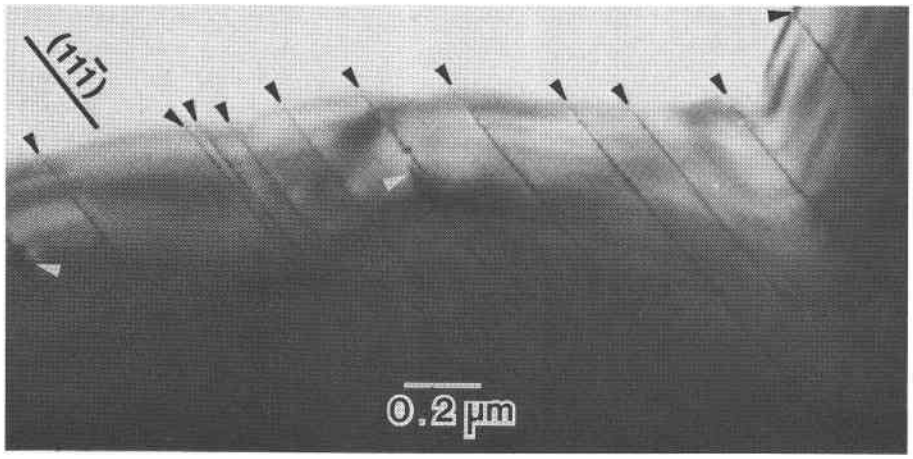

Fig. 6. Johannsenite with very narrow pyroxenoid lamellae (arrowed) parallel to (11$\bar{1}$) of the pyroxene. Two lamellae that terminate are indicated by white arrows.

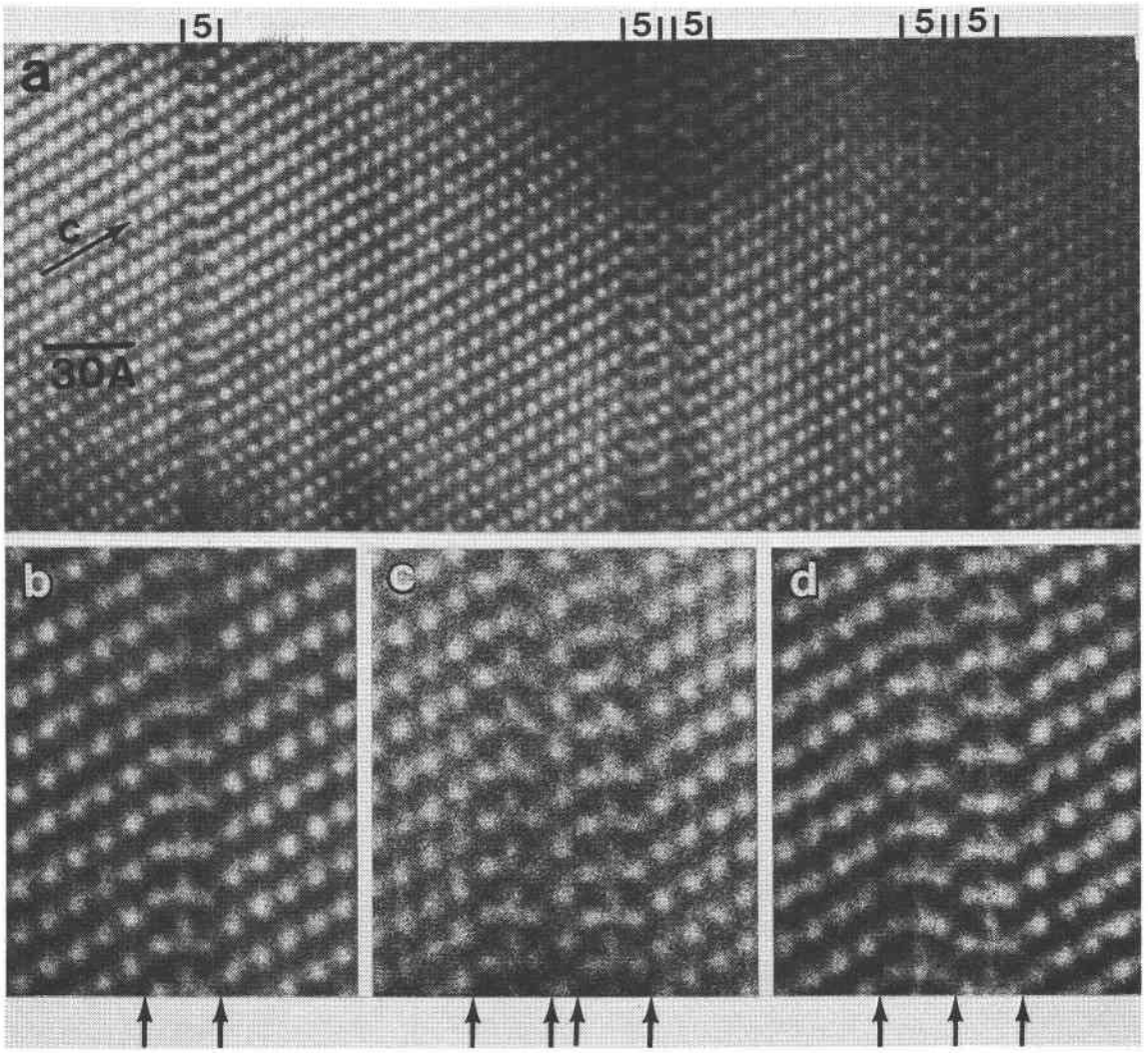

Fig. 7. HRTEM images of rhodonite lamellae in johannsenite. a. An area containing five rhodonite units (5). b. An enlarged view of an isolated rhodonite unit. The positions of the chain offsets are arrowed, c, d. Examples of paired rhodonite units. In c, there are four chain offsets, but in d, there are only three.

planar displacive faults in both pyroxenoids near the termination of the rhodonite lamella.

Bulk reactions

In contrast to the occurrence of relatively narrow pyroxenoid lamellae in the pyroxene, in some places pyroxenoid with disordered chain periodicity was observed to contact the johannsenite along more normal grain boundaries. This texture is illustrated in Figure 15, where the boundary is tilted with respect to the electron beam; the apparent width of the boundary increases with the thickness of the specimen, toward the lower left. The modulation of contrast along the boundary is a moiré effect resulting from the overlapping of pyroxene and pyroxenoid structures (a similar contrast effect on a pyroxene-amphibole grain boundary is shown in Veblen and Buseck, 1981, Fig. 15). The pyroxenoid in Figure 15 contains chain periodicities of five, seven, and nine, with a region of ordered pyroxmangite (seven). In all cases where such boundaries were observed between pyroxene and pyroxenoid, $(11\bar{1})$ of pyroxene was parallel to (001) of pyroxenoid, the same orientation relationship observed for the narrow pyroxenoid lamellae in pyroxene.

Boundaries between disordered pyroxenoid and pyroxene imply a mechanism of reaction different from the lamellar mechanisms discussed above. Instead, they indicate a bulk reaction mechanism, in which the pyroxenoid replaces pyroxene along a broad reaction front. Boundaries such as that in Figure 15 were observed to be quite continuous, in some cases being traceable for several microns

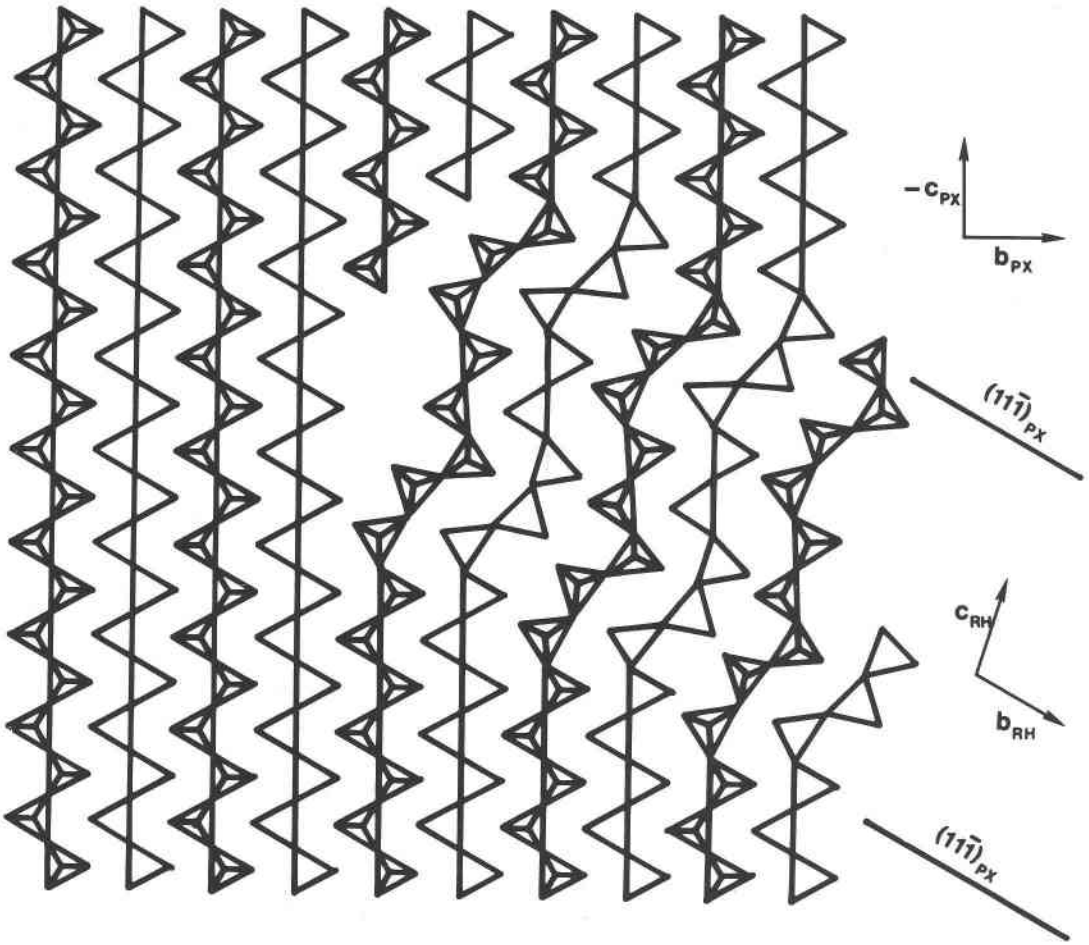

Fig. 8. A schematic projection normal to (100) of a terminating rhodonite slab injected into pyroxene structure. Only the silicate chains are shown. Slabs such as this one, with two chain offsets, can terminate in pyroxene without major structural distortions or planar faults associated with the termination.

before entering parts of the specimen too thick for observations. It is possible for a continuum to exist between lamellar and bulk reaction mechanisms, since a reaction lamella can be a single pyroxenoid unit wide or many units wide. Nevertheless, the bulk reaction behavior that produces broad reaction fronts like that of Figure 15 is clearly very different from the narrow lamellar behavior that produces textures such as that shown in Figure 6.

Discussion

Comparison with other mineral replacement reactions

As detailed above, the reaction of pyroxene to pyroxenoids was observed to take place by at least two different mechanisms, one involving the nucleation and growth of narrow pyroxenoid lamellae and the other involving replacement of the pyroxene along a broad reaction front. The presence of multiple reaction mechanisms in a single specimen is not, however, restricted to the present occurrence. Indeed, analogous behavior occurs in other solid-state replacement reactions involving chain silicates, as well as in other systems.

As shown by Veblen and Buseck (1980, 1981) and Veblen (1981), multiple mechanisms can operate in the replacement of pyroxene by amphibole and other biopyriboles and in the replacement of amphibole by wide-chain silicates, for example. Just as in the present case, these reactions can occur by the nucleation and growth of lamellae that are one or a few structural units wide, by the cooperative nucleation and growth of two or more lamellae separated by planar faults, and by bulk reaction mechanisms involving replacement along broad reaction fronts. Likewise, in all these cases there may be substantial variation in the reaction products, as well as the mechanisms. (For some of the reaction relationships in pyriboles, see Fig. 28 of Veblen and Buseck, 1981.)

Based on present knowledge from several systems, it is

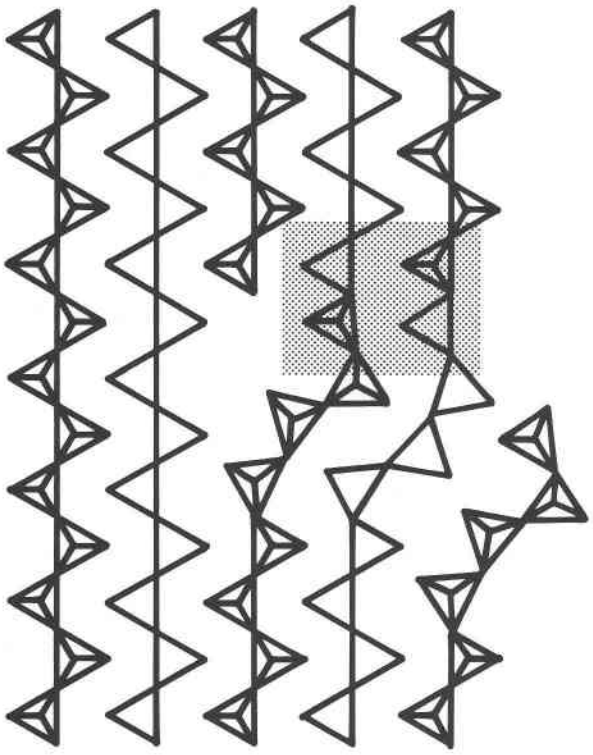

Fig. 9. A schematic projection normal to (100) of a single chain offset terminating in pyroxene. The silicate chains are discontinuous in the shaded area. This sort of structure can be expected to be unstable compared to structures such as that of Fig. 8, with paired offsets.

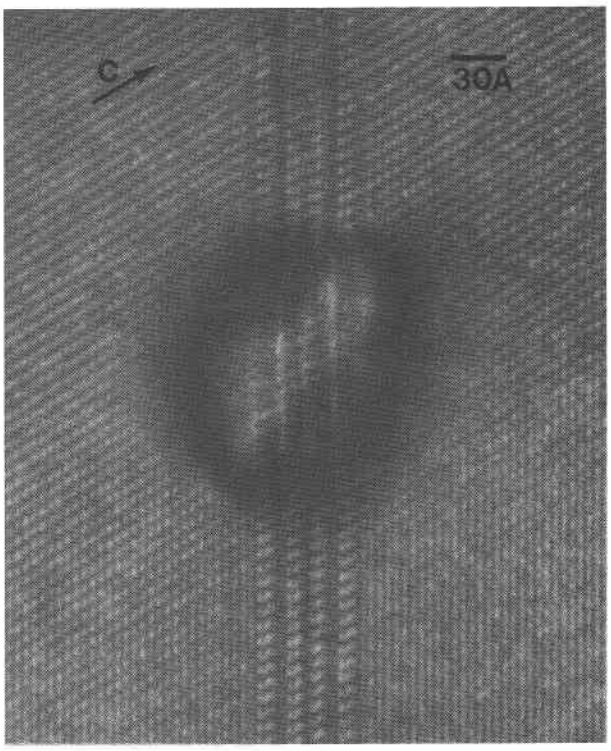

Fig. 10. Intense local strain contrast along a pyroxenoid lamella in johannsenite. Contrast in the vicinity of the fault is not interpretable in terms of a specific defect model.

possible to make a number of generalizations about replacement reactions in minerals, as follows:

1. There can be multiple paths by which a reaction can take place. In the present case, for example, we have seen that pyroxene may be replaced by either ordered rhodonite or pyroxmangite; these are different reaction paths.

2. For a given reaction path, there may be multiple mechanisms of reaction. For example, chain-periodicity disordered pyroxenoid can form from pyroxene by either lamellar or bulk mechanisms.

3. The relationships between the crystal structures of the parent and product phases in a replacement reaction can exercise a powerful control on the reaction behavior. Thus, in cases where the two structures can fit together coherently, as commonly occurs with structures that belong to a polysomatic series, lamellar reaction mechanisms are observed, and topotactic (three-dimensionally oriented) replacement by bulk mechanisms is also common. In the more general case, however, where the two structures are not closely related and do not mesh together in a particularly favorable way, replacement mechanisms involving extremely narrow lamellae are expected to be precluded by the resulting high interface energies. Likewise, topotactic and epitaxial bulk mechanisms will be less common, because specific orientation relationships are not favored by greatly reduced interface energies. Thus, in the general case, we expect the reactant phase or phases to be consumed by a bulk mechanism operating along a reaction front (i.e., at a grain boundary), with no special orientation relationships with the product phase or phases. This situation describes the ordinary type of heterogeneous solid-state reactions that occur in rocks during metamorphism, for example.

4. Minerals that have been replaced or partially replaced by lamellar reactions commonly are not ideal, homogeneous materials. Instead, "crystals" that have been replaced by such mechanisms may be complex mixtures of several minerals, structurally ordered and disordered, on an extremely fine scale. This is clearly true in the present case, where finely intergrown ordered pyroxene, rhodonite, and pyroxmangite occur with faulted material, as well as with disordered hybrid structures exhibiting a range of average structures. This is also true of the products of biopyribole replacement reactions cited above.

5. In replacement reactions in which the chemical composition of the product phase is different from that of the reactant, the chemical diffusion necessary for the reaction to proceed need not rely on bulk diffusion mechanisms,

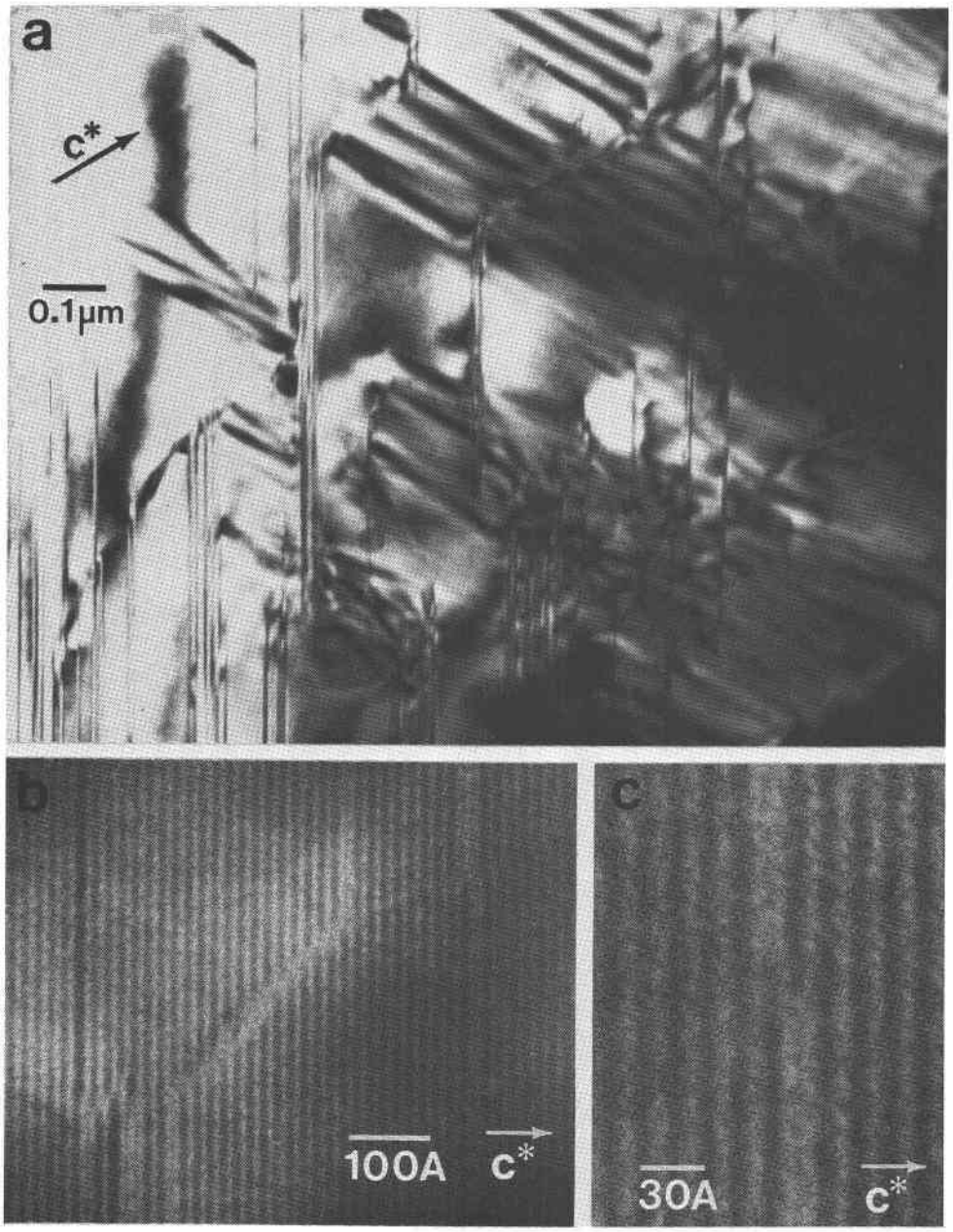

Fig. 11. a. Pyroxenoid lamellae in pyroxene (sharp vertical features) with terminations that are connected by planar faults (diffuse banded contrast like that typical of stacking faults). b. A planar fault in pyroxmangite at which chain periodicity faults (vertical) terminate. c. A localized displacive fault in pyroxmangite at which an elferketten unit (non-periodic vertical feature) is offset.

such as vacancy hopping. Instead, there may be rapid diffusion paths at the advancing tips of lamellae of the new phase or along the disordered interfaces that move through a crystal during a bulk reaction. This is not to say that bulk diffusion cannot occur during lamellar or bulk replacement reactions, but simply that it is not required by the geometry of the reacting system.

Observed reaction paths and the relevance of (Mn, Ca)SiO_3 phase relations

There have been several studies, on both synthetic and natural systems, relevant to the phase relations of Mn-Ca chain silicates. Taken together, these studies indicate that in coexisting rhodonite and pyroxmangite with Fe, Mg as

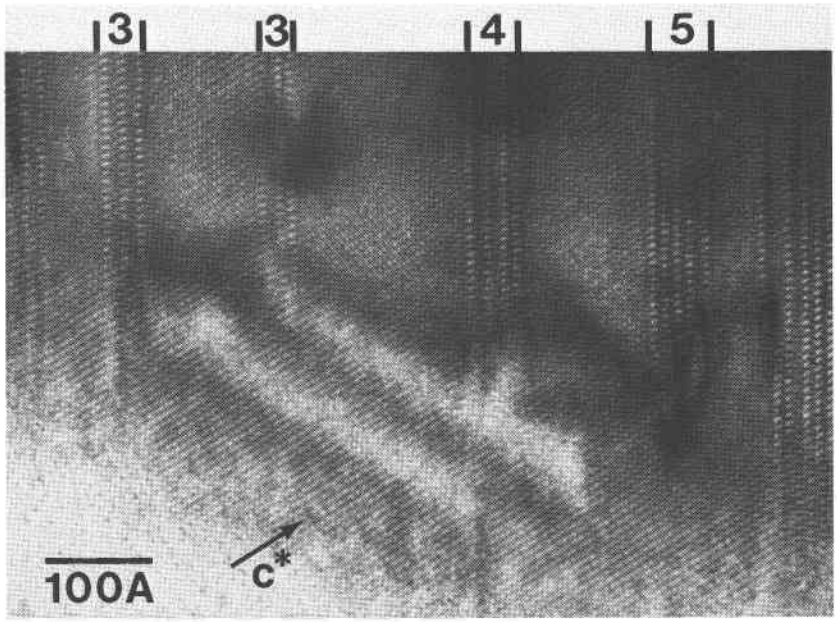

Fig. 12. Cooperatively terminating pyroxenoid lamellae in johannsenite. The lamellae terminate at planar defects (amorphous gray contrast), at which preferential electron radiation damage occurs. The numbers at the top refer to the numbers of pyroxneoid units in each lamella.

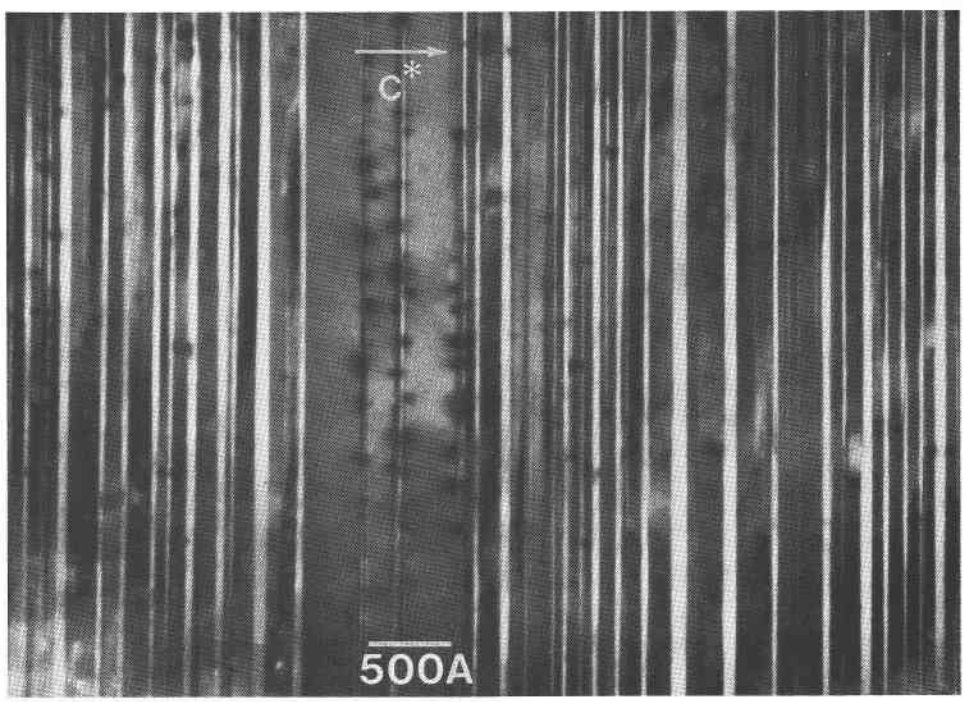

Fig. 13. Lamellar intergrowth of pyroxmangite and rhodonite (gray) with remnant pyroxene (white vertical stripes). Electron radiation damage (darker spots) has nucleated on the lamellar interfaces, probably as a result of strain. The c* direction refers to a pyroxenoid unit cell setting.

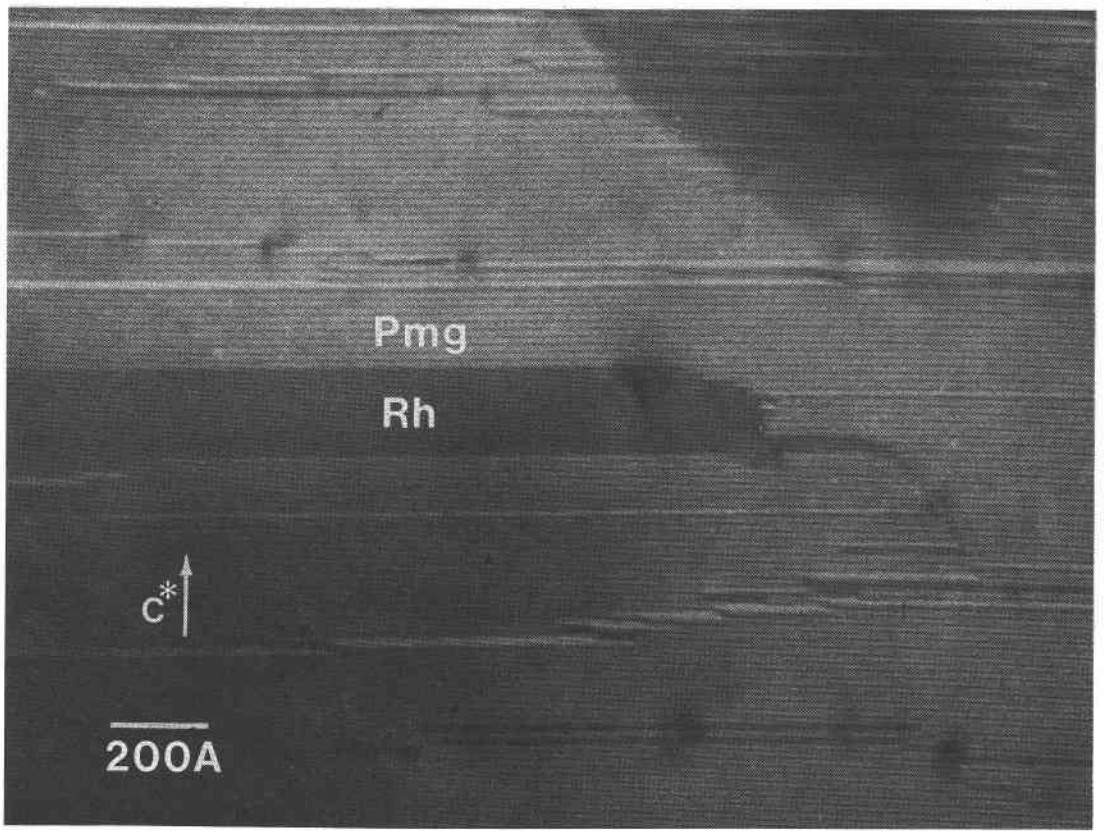

Fig. 14. Intergrown pyroxmangite and rhodonite from the area shown in Fig. 13. The rhodonite lamella near the center terminates in pyroxmangite with associated faults. Chain periodicity faults (non-periodic horizontal features) terminate or are offset in several places. The dark region in the upper right is heavily faulted.

low as in the present case, the rhodonite invariably contains more Ca than the pyroxmangite; a polymorphic relationship exists between rhodonite and pyroxmangite of the same composition, with rhodonite the high-temperature, low-pressure phase (Ito, 1972; Akimoto and Syono, 1972; Momoi, 1974; Ohashi et al., 1975; Abrecht and Peters, 1975; Maresch and Mottana, 1976; Peters et al., 1978).

From these relationships, with removal of Ca from the system we might expect a sequence of reactions from johannsenite to rhodonite to pyroxmangite, as diagrammed below the schematic binary composition diagram in Figure 16. Instead, as shown above the join in Figure 16, we observe that johannsenite has reacted directly to both rhodonite and pyroxmangite (and, although not shown in the figure, also to disordered mixtures of fünferketten and siebenerketten, which could be expected to have intermediate compositions). Following this initial set of reactions, the mixture of remnant pyroxene and the pyroxenoids is converted to the gemmy pink pyroxenoid, which is predominantly rhodonite. This indicates that much of the pyroxmangite that formed during the initial reactions ultimately was converted to rhodonite.

Since rhodonite is the higher-temperature phase, it cannot be argued that the rhodonite replaced pyroxmangite as a result of reactions during cooling from the peak metamorphic temperature. Instead, the most likely interpretation of the observed reaction paths is that the pyroxmangite and disordered mixed pyroxenoids formed metastably in the rhodonite stability field. They were subsequently converted to the stable phase, rhodonite. Perhaps the gemmy pink rhodonite grew as we now see it, with some intergrown pyroxmangite and chain periodicity disorder. It is also possible, however, that it grew as well-ordered rhodonite, replacing the pyroxmangite and disordered pyroxenoid, and was partially converted back to pyroxmangite during cooling. This question cannot be resolved by the present study. We can, however, ask why metastable pyroxmangite would have grown from johannsenite, rather than rhodonite. It is possible that this occurred because the structure of pyroxmangite is closer to that of johannsenite in the sense that it contains fewer chain offsets than rhodonite. Growth of pyroxmangite might therefore be kinetically favored because it requires less structural rearrangement of the pyroxene structure than replacement by rhodonite.

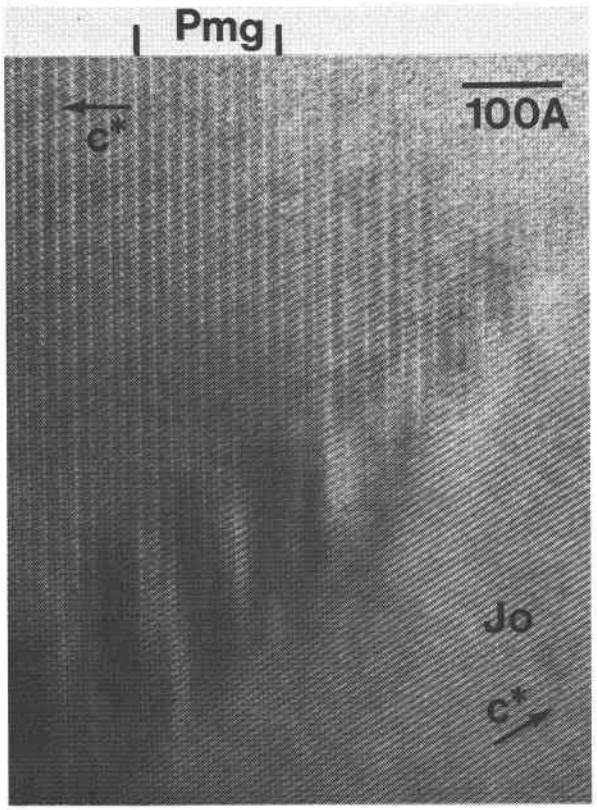

Fig. 15. A bulk reaction front between johannsenite and disordered pyroxenoid. The specimen thickens toward the lower left, so that the apparent width of the tilted interface increases. An ordered region of pyroxmangite is labelled Pmg.

The above speculations are based in part on the assumption that the pyroxmangite in this specimen contains less calcium than the rhodonite, as is normal. An analytical TEM study to resolve this question is in progress and will be reported in detail elsewhere. Initial results suggest that the rhodonite and pyroxmangite have very similar compositions. It is hoped that this study also will show whether the johannsenite reacted to pyroxenoids only after loss of substantial calcium and will determine the calcium-poor compositional limit for the pyroxene in this process.

Atomic mechanisms of reaction and dense-zone preservation

The structural aspects of solid-state transformations between pyroxenes and pyroxenoids have been examined in several studies. The transformations have been polymorphic in all cases (i.e., the reactant and product chain silicate have the same chemical composition) and have included rhodonite to "wollastonite" (Dent Glasser and Glasser, 1961; Prewitt and Peacor, 1964); johannsenite to bustamite (Morimoto et al., 1966); and pyroxmangite to rhodonite (Aikawa, 1979). While Dent Glasser and Glasser (1961) suggested that only silicon atoms must migrate during such a reaction, based on orientation relationships of the reactant and product unit cells, the subsequent authors have generally agreed that there also must be migration of at least some of the octahedrally coordinated cations.

The electron microscopic results reported here shed little light on the precise atomic motions during pyroxene–pyroxenoid reactions. As discussed for the replacement of pyroxenes by other pyriboles (Veblen and Buseck, 1981), the resolution of the present observations does not permit experimental verification of mechanisms below the large atomic cluster scale, and any discussion of atomic-scale mechanisms would be purely speculative.

Although atomic mechanisms are not accessible, the present observations, combined with the insights inherent in the polysomatic model for pyroxene–pyroxenoid structures, do help to explain the orientation relationships observed in reactions of pyroxene to pyroxenoid and between pyroxenoids with different chain periodicity. Morimoto et al. (1966) and Aikawa (1979) have rationalized these orientation relationships with the idea that a "dense zone" of cations is preserved in the transformations. While this appears to be correct in the geometrical sense that both reactant and product have these dense zones in common, it should be noted that the lamellae of pyroxenoid in the present case cut across the dense zones (the lamellae form parallel to $\{11\bar{1}\}$ of johannsenite, cutting across the dense zones [012] and [$0\bar{1}2$]). It is therefore most likely that the cations in the dense zones are rearranged at the tips of the growing pyroxenoid lamellae. Thus, in the strictest sense the dense zones may not truly be preserved, but rather are broken up and then reconstructed in the transformation.

What, then, controls the reaction mechanisms and the orientation relationships that are observed in solid state transformations between pyroxenes and pyroxenoids? As in reactions in other polysomatic structures, noted above, the reaction lamellae form parallel to planes of polysomatic slabs (Koto et al., 1976; Thompson, 1978). These are orientations of minimal strain between host and lamellae, and

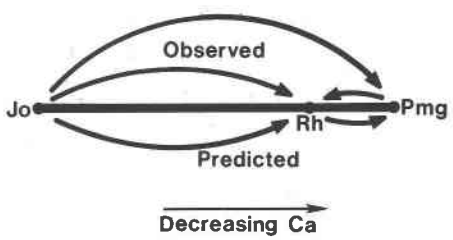

Fig. 16. Schematic composition diagram for Ca–Mn chain silicates, with Ca decreasing to the right. When coexisting, pyroxmangite is observed to contain less Ca than rhodonite. The expected path for an isothermal reaction involving loss of Ca is diagrammed below the binary composition line (johannsenite to rhodonite to pyroxmangite). The observed behavior, with johannsenite reacting to both rhodonite and pyroxmangite, followed by conversion of pyroxmangite to rhodonite, is shown above the line.

the reaction lamellae presumably form in these orientations for that reason. Viewed from this perspective of the polysomatic model for these chain silicates, we can rationalize the orientation relationships between reactant and product without resorting to the notion of dense zone preservation. Instead, these relationships can result simply from the requirement that the reactant and product structures must share a common orientation of W and P slabs, in order to minimize strain energy of the reaction intergrowths. In this view, dense zone preservation is simply a necessary consequence of the reaction mechanism, rather than the guiding principle for the reaction.

Orientational selectivity of the reactions

One curious observation of this study is that in most regions of pyroxene that have partially reacted, the pyroxenoid lamellae are parallel to only one of the two symmetry-equivalent $\{11\bar{1}\}$ pyroxene planes. This phenomenon is illustrated by Figure 13, which shows only one set of intergrown pyroxene and pyroxenoid lamellae. Were it present, the symmetry-related set of lamellae would also be visible in this orientation, although the lamellae would appear more diffuse because they would not be perfectly parallel to the electron beam. Areas several tens of microns in extent have been observed in the TEM to have only one lamellar orientation, and areas a few hundred microns across have been observed in petrographic thin sections to have only one orientation of optically resolvable lamellae. Contrary to these observations are those of Morimoto et al. (1966), who observed the expected two pyroxenoid orientations related by a mirror parallel to (010) in bustamite that was experimentally inverted from johannsenite.

Although only one set of pyroxenoid lamellae generally is present over relatively large regions of the specimen investigated in this study, there are exceptions to this observation. A region containing both the $(11\bar{1})$ and $(1\bar{1}\bar{1})$ orientations is shown in Figure 17, where the $(11\bar{1})$ set is in sharp contrast (parallel to the electron beam) and the $(1\bar{1}\bar{1})$ set of terminating lamellae appears as more diffuse wedges (tilted with respect to the beam). Also shown are other planar faults ("s"), which connect the terminations of lamellae in $(11\bar{1})$ orientation, and two other defects that are probably dislocations ("d").

Another possible exception to the typical observation of only one lamellar set is found in areas where there are many cooperatively terminating chain periodicity faults that are connected by other planar faults (Fig. 11a, for example). The precise nature of these other, connecting faults is difficult to ascertain, as pointed out by Ried and Korekawa (1980), because their orientations can vary and because they are not in an orientation that would permit high-resolution imaging studies. However, based on the work of Czank (1981), Czank and Liebau (1980), and Ried and Korekawa (1980), it seems likely that these faults are also chain periodicity faults, except where they are parallel to the pyroxene c-axis, in which case they would be stacking faults (by definition, a planar fault is a stacking fault when the fault vector is parallel to the plane of the fault, and it is a polysomatic fault when the fault vector lies outside the fault plane). The trace of the faults in Figure 11a, for example, is consistent with a second set of lamellae parallel to $(1\bar{1}\bar{1})$.

Even though there are the above exceptions, the overwhelming part of the pyroxene in this specimen that contains pyroxenoid lamellae has them in only one of two

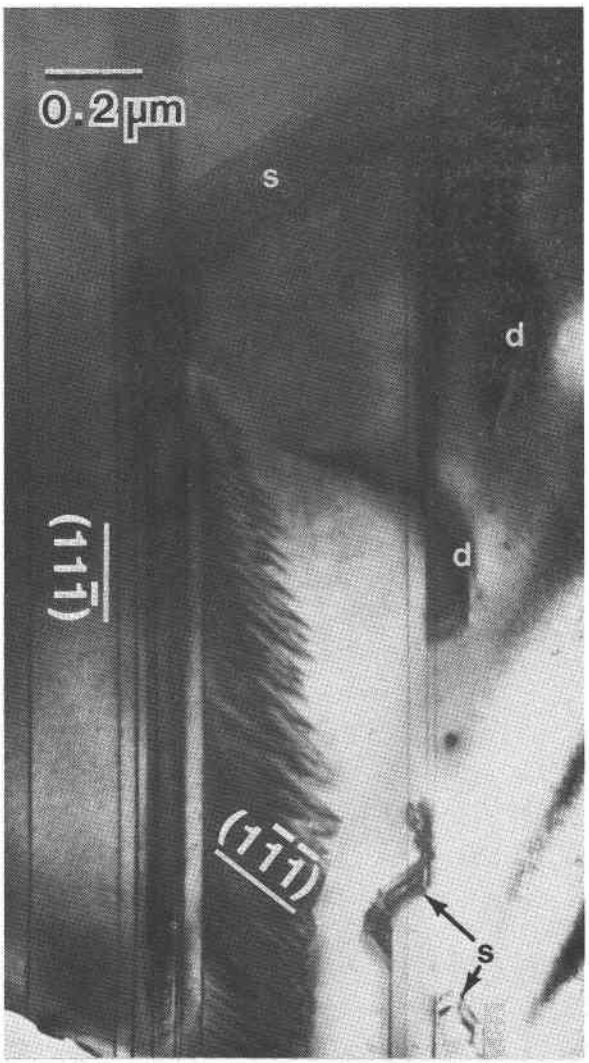

Fig. 17. An area where reaction to pyroxenoid in both of the symmetry-equivalent orientations $(11\bar{1})$ and $(1\bar{1}\bar{1})$ has occurred. The vertical $(11\bar{1})$ lamellae are parallel to the electron beam and are therefore in sharp contrast. The set of $(1\bar{1}\bar{1})$ lamellae is tilted with respect to the electron beam, so that they are in more diffuse contrast. These lamellae are wedge-shaped because they terminate. Planar faults (s) connect terminations of some of the $(11\bar{1})$ lamellae, and the two faults labelled d are probably dislocations.

symmetrically equivalent orientations. This behavior is similar to that of calcian dolomites, where Reeder (1981) observed that ordering occurs in only one of three symmetrically equivalent planes; of cordierite, where Putnis and Bish (1983) noted that Al–Si ordering occurs in a subset of several symmetrically equivalent orientations; and of wonesite, where exsolution of talc lamellae takes place in only one of two planes that are equivalent by the symmetry of the host (Veblen, 1983).

This orientational selectivity, which breaks the symmetry of the precursor phase, is not understood. It is possible that in some cases (wonesite, for example) an externally-applied stress forces the reaction process into a subset of the symmetrically equivalent orientations. Another possibility is that the primary structure may have lower symmetry than it is believed to possess. It is also possible that once a reaction process has been initiated by random choice in one orientation, a strain field (for example) that is produced by introduction of the reactant phase or phases forces that orientation to be obeyed by further reaction processes in the general neighborhood. The possible role of strain and partial dislocations in the observed orientational selectivity is discussed further by Angel et al. (1984) in their theoretical discussion of pyroxene–pyroxenoid reactions.

Another possible explanation for the orientational selectivity exhibited by the pyroxenoid lamellae in pyroxene is that they formed in the same orientation as a result of a templating mechanism. It is possible, for example, that the lamellae all nucleated at grain boundaries between pyroxene crystals and that the structures of these grain boundaries strongly favored nucleation in a single orientation. Alternatively, some pyroxenoid in specific orientations may have formed initially in the grain boundary regions by a bulk replacement mechanism. This first-formed pyroxenoid would then provide a template for the later narrow pyroxenoid lamellae that reacted into johannsenite.

Conclusions

This paper has described the microstructures that result from the reaction of a pyroxene to a complex mixture of both ordered and disordered pyroxenoids, which is finally replaced by relatively well-ordered rhodonite. This set of reactions is similar in many ways to solid-state replacement reactions that have been observed in other silicate minerals. For example, the reaction is not a simple replacement, but can instead follow several different paths, with both lamellar and bulk reaction mechanisms possible for each reaction path. The relationships among the crystal structures of the reactant and the products exercise controls on the reaction paths and mechanisms, and the material in which the reaction did not go to completion is a complex, submicroscopic mixture of several phases.

Several problems have been left unresolved by this study. First, it is not understood why johannsenite in some areas reacts first to pyroxmangite and then to rhodonite, since pyroxmangite generally contains less calcium than coexisting rhodonite. Similarly, it is not known whether calcium loss in the pyroxene precedes the nucleation and growth of the pyroxenoids. These questions will be clarified by a thorough analytical TEM investigation. Finally, we do not understand the orientational selectivity exhibited by this reaction, in which pyroxenoid lamellae typically form in only one of two symmetrically equivalent orientations over relatively large regions. The most likely explanation for this phenomenon appears to be some sort of templating mechanism or the involvement of strain.

Acknowledgments

Prof. Donald M. Burt first observed these pyroxene-pyroxenoid intergrowths and kindly provided the specimen for TEM study. I thank Nancy Honce and Gerard Spinnler for assisting in the early X-ray experiments. Helpful reviews were provided by Drs. R. J. Angel, Michael Czank, Yoshikazu Ohashi, and Donald Peacor. This work was supported by NSF grant EAR83-06861. Electron microscopy was performed at the Arizona State University Facility for HREM and The Johns Hopkins University high-resolution electron microscope laboratory, which were established with support from NSF grants CHE79-16098 and EAR83-00365 respectively.

References

Abrecht, J. and Peters, Tj. (1975) Hydrothermal synthesis of pyroxenoids in the system $MnSiO_3$-$CaSiO_3$ at Pf = 2 kb. Contributions to Mineralogy and Petrology, 50, 241–246.

Aikawa, Nobuyuki (1979) Oriented intergrowth of rhodonite and pyroxmangite and their transformation mechanism. Mineralogical Journal, 9, 255–269.

Aikawa, Nobuyuki (1984) Lamellar structure of rhodonite and pyroxmangite intergrowths. American Mineralogist, 69, 270–276.

Akimoto, S. and Syono, Y. (1972) High pressure transformation in $MnSiO_3$. American Mineralogist, 57, 76–84.

Alario Franco, M., Jefferson, D. A., Pugh, N. J., and Thomas, J. M. (1980) Lattice imaging of structural defects in a chain silicate: the pyroxenoid mineral rhodonite. Materials Research Bulletin, 15, 73–79.

Angel, R. J., Price, G. D., and Putnis, Andrew (1984) A mechanism for pyroxene-pyroxenoid and pyroxenoid-pyroxenoid transformations. Physics and Chemistry of Minerals, 10, 236–243.

Burnham, C. W. (1966) Ferrosilite III: A triclinic pyroxenoid-type polymorph of ferrous metasilicate. Science, 154, 513–516.

Buseck, P. R. and Cowley, J. M. (1983) Modulated and intergrowth structures in minerals and electron microscope methods for their study. American Mineralogist, 68, 18–40.

Buseck, P. R., Nord, G. L., Jr., and Veblen, D. R. (1980) Subsolidus phenomena in pyroxenes. In C. T. Prewitt, Ed., Pyroxenes, Mineralogical Society of America Reviews in Mineralogy, 7, 117–211.

Catlow, C. R. A., Thomas, J. M., Parker, S. C., and Jefferson, D. A. (1982) Simulating silicate structures and the structural chemistry of pyroxenoids. Nature, 295, 658–662.

Cowley, J. M. (1975) Diffraction Physics. North-Holland Publishing Company, Amsterdam.

Czank, Michael (1981) Chain periodicity faults in babingtonite, $Ca_2Fe^{2+}Fe^{3+}H[Si_5O_{15}]$. Acta Crystallographica, A37, 617–620.

Czank, Michael and Liebau, Friedrich (1979) Periodizitätsfehler in Pyroxenoiden—eine neue Art von Baufehlern (elektronenmikroskopische Untersuchungen). Fortschritte der Mineralogie, 57, 23–24.

Czank, Michael and Liebau, Friedrich (1980) Periodicity faults in chain silicates: a new type of planar lattice fault observed with high resolution electron microscopy. Physics and Chemistry of Minerals, 6, 85–93.

Czank, Michael and Simons, Bruno (1983) High resolution electron microscopic studies on ferrosilite III. Physics and Chemistry of Minerals, 9, 229–234.

Dent Glasser, L. S. and Glasser, F. P. (1961) Silicate transformations: rhodonite-wollastonite. Acta Crystallographica, 14, 818–822.

Iguchi, E. and Tilley, R. J. D. (1978) The elastic strain energy of crystallographic shear planes in ReO_3-related oxides. II. *CS* plane arrays. Journal of Solid State Chemistry, 24, 131–141.

Ito, Jun (1972) Rhodonite-pyroxmangite peritectic along the join $MnSiO_3$ in air. American Mineralogist, 57, 865–876.

Jefferson, D. A. and Pugh, N. J. (1981) The ultrastructure of pyroxenoid chain silicates. III. Intersecting defects in a synthetic iron-manganese pyroxenoid. Acta Crystallographica, A37, 281–286.

Koto, Kichiro, Morimoto, Nobuo, and Narita, Hajime (1976) Crystallographic relationships of the pyroxenes and pyroxenoids. Journal of the Japan Association of Mineralogists, Petrologists, and Economic geologists, 71, 248–254.

Liebau, Friedrich (1962) Die Systematik der Silikate. Naturwissenschaften, 49, 481–491.

Liebau, Friedrich (1980) Classification of silicates. In P. H. Ribbe, Ed., Orthosilicates, Mineralogical Society of America Reviews in Mineralogy, 5, 1–24.

Maresch, W. V. and Mottana, A. (1976) The pyroxmangite–rhodonite transformation for the $MnSiO_3$ composition. Contributions to Mineralogy and Petrology, 55, 69–79.

Momoi, H. (1974) Hydrothermal crystallization of $MnSiO_3$ polymorphs. Mineralogical Journal, 7, 359–373.

Morimoto, Nobuo, Koto, Kichiro, and Shinohara, T. (1966) Oriented transformation of johannsenite to bustamite. Mineralogical Journal, 5, 44–64.

Narita, Hajime, Koto, Kichiro, and Morimoto, Nobuo (1977) The crystal structures of $MnSiO_3$ polymorphs (rhodonite- and pyroxmangite-type). Mineralogical Journal, 8, 329–342.

Ohashi, Yoshikazu and Finger, L. W. (1975) Pyroxenoids: a comparison of refined structures of rhodonite and pyroxmangite. Carnegie Institution of Washington Year Book, 74, 564–569.

Ohashi, Yoshikazu, Kato, Akira, and Matsubara, S. (1975) Pyroxenoids: a variation in chemistry of natural rhodonites and pyroxmangites. Carnegie Institution of Washington Year Book, 74, 561–564.

Peters, Tj., Trommsdorff, V., and Sommerauer, J. (1978) Manganese pyroxenoids and carbonates: critical phase relations in metamorphic assemblages from the Alps. Contributions to Mineralogy and Petrology, 66, 383–388.

Prewitt, C. T. and Peacor, D. R. (1964) Crystal chemistry of the pyroxenes and pyroxenoids. American Mineralogist, 49, 1527–1542.

Putnis, Andrew and Bish, D. L. (1983) The mechanism and kinetics of Al, Si ordering in Mg-cordierite. American Mineralogist, 68, 60–65.

Reeder, R. J. (1981) Electron optical investigation of sedimentary dolomites. Contributions to Mineralogy and Petrology, 76, 148–157.

Ried, Holger (1984) Intergrowth of pyroxene and pyroxenoid; chain periodicity faults in pyroxene. Physics and Chemistry of Minerals, 10, 230–235.

Ried, Holger and Korekawa, M. (1980) Transmission electron microscopy of synthetic and natural fünferketten and siebenerketten pyroxenoids. Physics and Chemistry of Minerals, 5, 351–365.

Ried, Holger, Schropfer, L., and Korekawa, M. (1979) Synthese von Proxferoit und Fe-Rhodonit bei niedrigem Druck (<1 atm). Zeitschrift für Kristallographie, 149, 121–123.

Stoinova, M. and Pirov, T. (1974) The Govedarnika polymetallic deposit, District of Luki, Northern Rhodope Mountains. In Dragov, P. and Kolkovsik, B., Eds., Twelve Ore Deposits in Bulgaria, International Association on the Genesis of Ore Deposits (IAGOD), Fourth Symposium, Varna, Bulgaria, 134–148.

Sundius, N. (1931) On the triclinic manganiferous pyroxenes. American Mineralogist, 16, 411–429.

Takéuchi, Yoshio and Koto, Kichiro (1977) A systematics of pyroxenoid structures. Mineralogical Journal, 8, 272–285.

Thompson, J. B., Jr. (1978) Biopyriboles and polysomatic series. American Mineralogist, 63, 239–249.

Veblen, D. R. (1981) Non-classical pyriboles and polysomatic reactions in biopyriboles. In D. R. Veblen, Ed., Amphiboles and Other Hydrous Pyriboles—Mineralogy, Mineralogical Society of America Reviews in Mineralogy, 9A, 189–236.

Veblen, D. R. (1982) Replacement of johannsenite by Mn-pyroxenoids: Microstructures and mechanisms of reaction (abstr.). Geological Society of America Abstracts with Programs, 14, 637.

Veblen, D. R. (1983) Exsolution and crystal chemistry of the sodium mica wonesite, American Mineralogist, 68, 554–565.

Veblen, D. R. and Buseck, P. R. (1979) Chain-width order and disorder in biopyriboles. American Mineralogist, 64, 687–700.

Veblen, D. R. and Buseck, P. R. (1980) Microstructures and reaction mechanisms in biopyriboles. American Mineralogist, 65, 599–623.

Veblen, D. R. and Buseck, P. R. (1981) Hydrous pyriboles and sheet silicates in pyroxenes and uralites: intergrowth microstructures and reaction mechanisms. American Mineralogist, 66, 1107–1134.

Manuscript received, January 11, 1983;
accepted for publication, May 1, 1985.